Journal of Sedimentary Research

Journal of Sedimentary Research, 2017, v. 87, 866–879
Research Article
DOI: http://dx.doi.org/10.2110/jsr.2017.52

INTERACTIONS OF A PALEOCENE RIVER, A RISING FOLD, AND EARLY-DIAGENETIC CONCRETIONS

DAVID B. LOOPE AND ROSS SECORD
Department of Earth & Atmospheric Sciences and University of Nebraska State Museum, University of Nebraska–Lincoln, Lincoln, Nebraska 68588-0340, U.S.A.
e-mail: dloope1@unl.edu

ABSTRACT: **The relative rates of sediment accumulation, erosion, and structural uplift determine whether a growing fold develops positive topographic relief, is beveled by antecedent streams, or is buried under thick growth strata. When folds rise in subsiding basins, upward, convergent flow of groundwater through the permeable growth strata that underlie antecedent streams enhances the flux of ions required for concretion growth. Early diagenetic concretions that grow in such alluvial strata may constitute the only clasts larger than sand size available for transport when antecedent streams become erosive. The first reworked concretions deposited by these streams should accurately mark the transition from aggradation to erosion as folds rise into the paths of streams. In this situation, the ability to differentiate reworked from *in situ* concretions is crucial.**

The west-vergent Simpson Ridge anticline, a N–S-trending, thick-skinned Laramide structure in east-central Wyoming, separates the larger Hanna basin from the Carbon basin. Near the north nose of this anticline, *in situ* iron-oxide-rich concretions are abundant in folded Paleocene strata (Ferris Formation) and, just to the east, large, reworked, iron-rich concretions are abundant in younger, more gently dipping conglomerates in the basal Hanna Formation of the backlimb. Smaller reworked concretions are also present near the base of the Hanna Formation at least 7 km south of the anticlinal nose and just east of the fold's axis.

At the anticlinal nose, *in situ* (non-reworked) concretions up to 3 m $\times$ 1 m $\times$ 1 m are abundant at the top of an $\sim$ 7-km-thick sequence of sandstones and siltstones that constitute the Late Cretaceous–early Paleocene Ferris Formation. Reworked concretions are absent in the strata hosting these *in situ* concretions, but reworked concretionary clasts up to 2 m in diameter are present in exposures of conglomerates in the lowermost Hanna Formation that lie just above the *in situ* Ferris concretions and southeast of the anticlinal nose. These early-diagenetic concretions were originally cemented by siderite ($FeCO_3$). Oxidation of some small, rinded siderite-cemented clasts took place after their fluvial transport into the Hanna Formation, but abundant angular, un-rinded, iron-oxide-cemented clasts indicate that many large, *in situ* siderite concretions had resided in the vadose zone before they were entrained. The distribution of reworked concretions and the orientations of crossbeds show that antecedent Hanna streams eroded a swath at least 5 km wide across the rising structure. These streams transported Ferris Formation concretions southeastward into the Carbon basin, and deposited them in a conglomeratic sandstone body in the Hanna Formation. Large calcite-cemented concretions, many with a pipe-like morphology, then grew within Hanna crossbeds. In many cases, these *in situ* concretions enclose transported, iron-rich concretions, but there is no evidence any calcite-cemented concretions were reworked. The NW–SE alignment of the pipes record southeastward flow of groundwater and thus also provide evidence (together with the orientation of the crossbeds) of the original continuity of the Hanna Formation across the anticline.

Reworked concretions reveal the interplay of deposition, diagenesis, and erosion. Due to convergent groundwater flow over growing anticlines, early diagenetic concretions, both *in situ* and as reworked clasts, are especially likely to be found in growth strata.

INTRODUCTION

Early diagenetic, siderite-cemented concretions are common in sedimentary rocks and can provide clues to paleoclimate, pore-water chemistry, and sedimentation rates (Gautier 1982; Mozley 1989; Ludvigson et al. 1998; Ludvigson et al. 2010). Like other products of early diagenesis, siderite concretions can be reworked into sedimentary lags by high-energy fluvial or marine processes (Fig. 1; Allen 1987; Pye et al. 1990). Although many geologists are sufficiently familiar with chert nodules and calcrete to recognize their reworked remains, siderite can be altered into iron-oxide-cemented forms that are less easily identified.

Siderite is unstable in the presence of O_2. Siderite concretions are fully preserved in outcrops of Cretaceous marine mudrocks on the western Great Plains of North America (Gautier 1982). The ions required for growth of these concretions came from the surrounding muddy sediment. In sandy sediment, the ions required for concretion growth can travel much greater distances (Loope and Kettler 2015). Those siderite concretions that grow in permeable sandstones and unconsolidated alluvium are likely to be altered to iron oxide when, due to tectonic uplift, they approach the land surface. In oxidizing, shallow groundwater, iron-oxidizing microbes can transform siderite concretions into dense iron-oxide rinds surrounding friable, iron-

Published Online: August 2017
 1527-1404/17/087-866/$03.00

FIG. 1.—One very large, calcite-cemented concretion (CC) that encloses dozens of large, reworked iron-oxide-cemented (formerly siderite) concretions. Crest of Halfway Hill (41° 48.939′ N; 106° 15.853′ W; WGS 84 datum).

poor interiors (van der Burg 1969; Loope et al. 2012), or into a combination of dense, iron-oxide-cemented bands and iron-oxide stain (true Liesegang; Kettler et al. 2015; Burgess et al. 2016). Large siderite concretions in sandstones are commonly fractured into small, three-dimensional compartments; oxidation along the fractures generates boxworks delineated by dense accumulations of iron oxide (Taylor 1949; Loope et al. 2011; Loope et al. 2012; Burgess et al. 2016).

In the greater Hanna basin of south-central Wyoming (Fig. 2), as much as 7 km of Upper Cretaceous to lower Eocene strata are present in the Ferris and Hanna formations. These rocks accumulated in the span of about 10 Myr (Lillegraven 2015) and are dominated by sandstones, siltstones, and shales, but also contain numerous lignites and coals. All previous authors have attributed the great thickness of the Ferris and Hanna formations to syndepositional tectonism, but there is considerable disagreement concerning the relationship between surface drainages and active structures (Ryan 1977; Lillegraven and Ostresch 1988; Wroblewski 2006; Lillegraven et al. 2004). Ferris strata accumulated near the western margin of the Cannonball Sea (Wroblewski 2006; Boyd and Lillegraven 2011), but fluvial strata and hiatuses in the Hanna Formation may record the sinuous pathway of the Paleogene "California River" (Davis et al. 2010) through Wyoming's Laramide uplifts on its way to the western Gulf of Mexico (Blum and Plecha 2014; Sharman et al. 2017). Lillegraven (2015) provided highly detailed geologic maps, cross sections, and voluminous field notes on the structure and stratigraphy of the eastern portion of the Greater Hanna basin, including most of the Carbon basin (Fig. 2) that have aided this study.

In this paper, after first setting the stratigraphic and tectonic framework, we focus on the origins and distributions of two kinds of iron-rich concretions, and then address their significance to changing rates of fluvial aggradation, erosion, and tectonic uplift. In our study area (Fig. 2), *in situ* iron-oxide-cemented (formerly siderite) concretions are laterally and stratigraphically widespread in the Ferris Formation. In the study area, the younger Hanna Formation contains abundant reworked, iron-oxide-cemented concretions near its base, as well as abundant *in situ* calcite-cemented concretions throughout its exposed thickness. After describing the spatial distributions and the similarities and differences between the *in situ* and the reworked concretions, we argue that the reworked concretions in the basal Hanna Formation were derived from nearby outcrops of the Ferris Formation as they were eroded during uplift along the Simpson Ridge anticline (now separating the Hanna and Carbon basins; Fig. 2). Although he did not recognize the reworked nature of the iron concretions that are the focus of this paper, Secord (1998) proposed a similar scenario. He suggested that some distinctive coarse-grained clasts (dark chert pebbles, silicified Paleozoic marine fossils, silicified wood) found in the basal Hanna Formation in the Carbon basin were reworked from the Ferris Formation by southeast-flowing rivers. He noted that pebble conglomerates found in the basal Hanna Formation were atypical of the Hanna Formation but resembled typical gravels of the Ferris Formation, especially as seen in outcrops on Hi Allen Ridge on the northern end of the Simpson Ridge anticline (Fig. 2).

The distribution of reworked iron concretions, together with data based on orientations of crossbeds and *in situ*, pipe-like concretions, show that both the Ferris and Hanna formations are composed of growth strata deposited during rise of the Simpson Ridge anticline (Fig. 3). Where rivers interact with growing folds, reworked early-diagenetic concretions may constitute the only large, durable clasts available for transport by antecedent streams. If present, these clasts can accurately (and prominently) mark the transition from aggradation to erosion as tectonic structures rise into the paths of fluvial systems. The geometry of permeable growth strata deposited in water gaps above impermeable pre-growth strata constrains both lateral and vertical flow in the unconfined aquifer (Fig. 3). This results in narrower flow bands and increased Darcy velocity above the constriction (Freeze and Cherry 1979, p. 21), making the growth strata especially favorable sites for concretion formation.

STRATIGRAPHIC AND TECTONIC SETTING

The Hanna and Carbon basins, relatively small structural basins located in southeastern Wyoming, were tectonically active from Late Cretaceous to middle Eocene time (Blackstone 1983, 1993; Merewether 1983; Love 1970; Lillegraven et al. 2004; Lillegraven 2015). Before widespread deformation in the Paleocene and middle Eocene, these basins were part of a much larger depositional basin including the Greater Green River Basin to the west and the Laramie basin to the east (Lillegraven et al. 2004; Lillegraven 2015). The Hanna and Carbon basins are now separated by the Simpson Ridge anticline, a west-vergent structure that plunges NNE and is exposed at the surface for about 25 km (Fig. 2). Wroblewski (2003) estimated the combined thickness of the Ferris and Hanna formations in the Hanna basin to be ten times their combined thickness in the adjacent

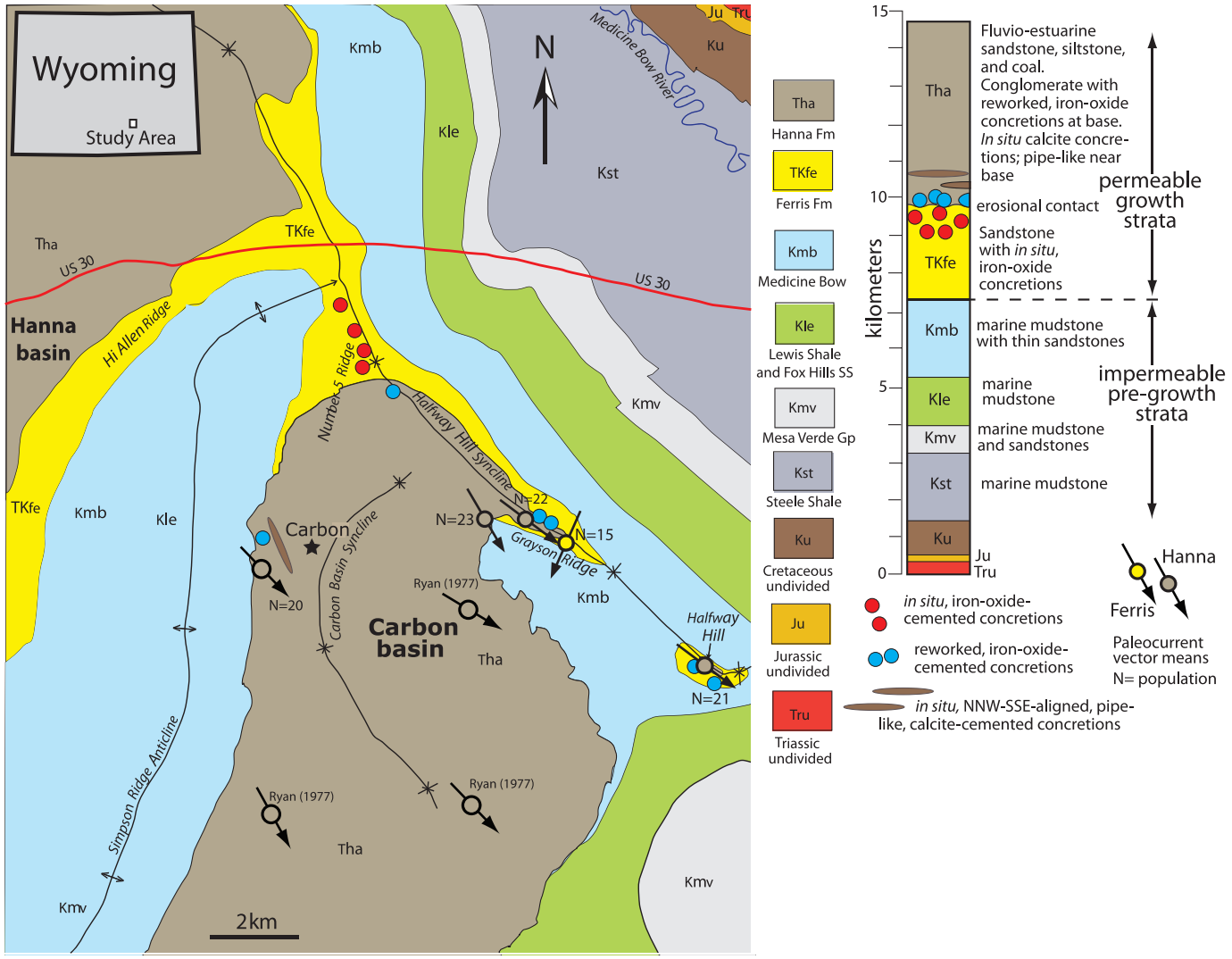

FIG. 2.—Geologic map and stratigraphic column of study area and vicinity. Colored dots and ellipses show distribution of studied concretions. Arrows with accompanying circles show mean orientations of trough cross-strata measured from the Hanna and Ferris Formations; three of the paleocurrent arrows are from Ryan (1977). Star marks the site of the former town of Carbon. Map is modified from Lillegraven (2015), his figure 5. Highly generalized column is based on Lillegraven's figure 2, and emphasizes features described in the text. Note that, due to localized tectonism, stratal thicknesses vary widely.

Carbon basin. The relative thinness of the Ferris–Hanna strata of the Carbon basin compared to their great thickness in the Hanna basin was largely due to high subsidence rates in the basin center and uplift of Simpson Ridge anticline (Wroblewski 2003). The Ferris and Hanna formations in the Carbon basin are separated by an erosional unconformity that may record the loss of thick strata or long periods of non-deposition. Lillegraven (2015) hypothesized that uplift of Simpson Ridge may have coincided with major erosional scouring of Carbon basin strata.

Various timing relations have been proposed for development of the Simpson Ridge anticline. Ryan (1977) stated that it was tectonically active during deposition of both the Ferris and Hanna formations (Lower Cretaceous through the Paleocene). Lefebre (1988) argued that Simpson Ridge became prominent during deposition of the Hanna Formation. According to Secord (1998), the primary formation of Simpson Ridge occurred in the early Paleocene after deposition of local lower Ferris Formation, but before deposition of local Hanna Formation. In contrast, Hansen (1986) and Lillegraven (2015) concluded that Simpson Ridge formed later, in the early or middle Eocene. The age of the Ferris Formation on Simpson Ridge is poorly constrained but, based on biochronologic ages of fossils in the northern Hanna basin, the Ferris Formation in the type area was deposited during the latest Cretaceous (Maastrichtian) and early Paleocene (Danian). Both Late Cretaceous dinosaur and Puercan (early Danian) mammal fossils are known from the Ferris Formation (Eberle and Lillegraven 1998a, 1998b). A similar age range for the Ferris Formation on Simpson Ridge is probable since the overlying Hanna Formation is not older than late Danian (assuming a depositional contact, see below).

Secord (1998) placed a partial age constraint on the folding of Simpson Ridge using mammalian fossils found in the northern Carbon basin in the basal Hanna Formation, which he interpreted as onlapping an already folded anticline. The Hanna Formation along the eastern margin of Simpson Ridge dips eastward by ~ 20–35 degrees (Lillegraven 2015, his fig. 5), which Secord interpreted as evidence for additional uplift following deposition of the basal Hanna Formation. Ryan (1977) suggested that the upper Ferris Formation was deposited by streams flowing around the north nose of the anticline, and that tilting of both the Ferris and the Hanna formations resulted from continuing growth of the anticline.

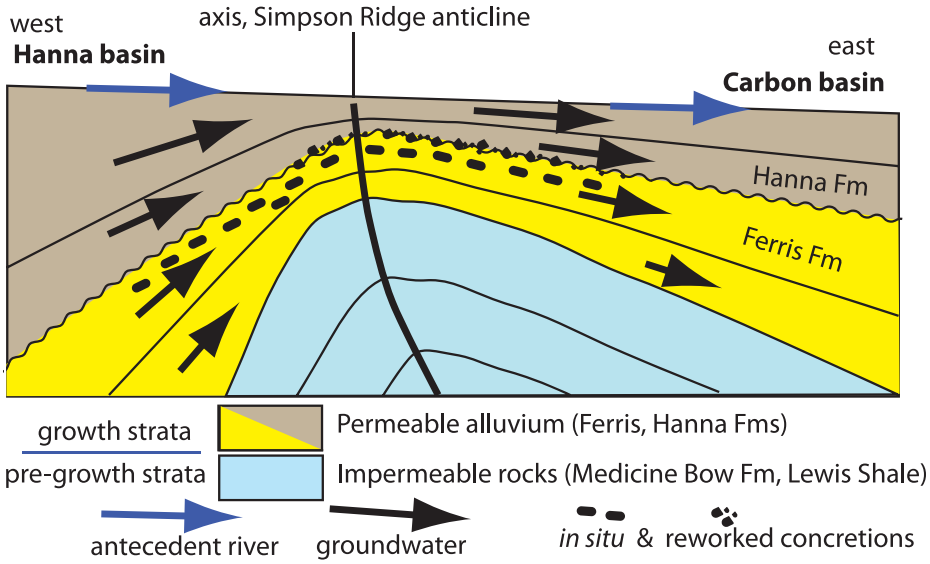

FIG. 3.—Interpretive cross section of the Simpson Ridge anticline showing relationships between the growing structure, stream flow, groundwater flow, and the distribution of *in situ* and reworked concretions. Growth strata were deposited by an eastward-flowing river system during active uplift of the structure. Vertical convergence of groundwater as it flowed across the structure increased the flux of ions and dissolved organic matter, enhancing concretion growth. Stratal thicknesses and lateral extents of *in situ* concretions are poorly constrained. Modified from Burbank et al. (1996); cf. Wroblewski (2003), his figure 7.

Mammalian fossils in the basal Hanna Formation in the northern Carbon basin at Grayson Ridge and Halfway Hill (Fig. 2) indicate an age close to that of the Torrejonian–Tiffanian North American land-mammal age boundary (Secord 1998). The boundary between these land-mammal ages lies very close to the C27n–C26r magnetochron reversal (Archibald et al. 1987; Lofgren et al. 2004), placing these rocks in the upper Danian (late early Paleocene) at ~ 62 Ma (Ogg 2012).

A significant intraformational unconformity low in the Hanna Formation, but above its base, was recognized by Secord (1998) based on mammal fossils that were collected from directly above and below a deeply channeled erosional surface at Halfway Hill. Lag deposits associated with this unconformity are darkly stained and contain abundant reworked iron concretions. Fossils above this surface constrain the age of these rocks to middle and/or late parts of the Tiffanian land-mammal age. Biostratigraphic revision of the Tiffanian (Secord et al. 2006; Secord 2008) since these fossils were first described suggests age equivalence to the Ti-4a or Ti-4b Tiffanian biozones of the Bighorn basin. *Arctocyon mumak*, which occurs above the intraformational Hanna unconformity, is known only from these zones in the Bighorn basin. Specimens of *Plesiadapis*, found stratigraphically lower (but still above the unconformity), could belong to species that are slightly older (*P. rex*), slightly younger (*P. fodinatus*), or age equivalent (*P. churchilli*) to *A. mumak*. Taken together, these fossils suggest age equivalence to the Ti-3 or Ti-4 biozones, which correlate to upper Selandian and earliest Thanetian stages respectively (Secord et al. 2006). This implies a hiatus of at least 1.2 Myr, and more probably 2 to 3 Myr (based on *A. mumak*) for the intraformational Hanna unconformity.

In agreement with the conclusions of Wroblewski (2003), we argue below that paleoflow indicators from sandstones (in both the Hanna and Carbon basins), the reworked concretions in Hanna Formation conglomerates east of the Simpson Ridge anticline, and widespread soft-sediment deformation in the Hanna Formation are all fully consistent with syntectonic control of drainage and accommodation. Gentle folding of the youngest Hanna Formation at Halfway Hill (Fig. 2) indicates that tectonism continued after deposition of the local Hanna Formation was had ceased.

Wroblewski (2003) recognized lacustrine deposits of middle Paleocene age in the central Hanna basin. He interpreted basal strata of the Hanna Formation in the Carbon basin (exposed along the axis of the Halfway Hill syncline; Fig. 2) as an erosional paleovalley, and he linked this valley to another paleovalley in the Hanna basin (upstream to the west) at a similar stratigraphic level.

Lillegraven (2015) argued that the Ferris Formation, deposited on both sides of the Simpson Ridge anticline, pre-dated uplift of that anticline. Higher on the limbs of this structure, Hanna Formation strata rest directly on steeply dipping mudstones of the Medicine Bow Formation; Lillegraven (2015) interpreted this contact as tectonic, rather than depositional, and proposed a provocative hypothesis: he mapped the entire Hanna Formation of the Carbon basin as a thick, 17-km-wide structural klippe (Fig. 2). Immediately east of the anticlinal axis, however, the Hanna Formation contains large, reworked concretions and rests upon a much thinner Ferris Formation. In the Discussion, we point out that the klippe hypothesis does not account for the source or stratigraphic distribution of the conglomerate that contains the reworked concretions, nor for the paleoflow indicators in the sandstones. We argue that such clasts, sedimentary structures, and spatial relationships, however, are to be expected where products of early diagenesis grow within the deposits of rivers that cross rising anticlines.

IN SITU, IRON-RICH CONCRETIONS IN THE FERRIS AND HANNA FORMATIONS

Description

Secord (1998), Hasiotis and Honey (2000), Lillegraven et al. (2004, p. 58–63), and Lillegraven (2015) have reported sideritic strata in the Hanna Formation. Lillegraven (2015, p. 63, 104) described an area that contains unusually iron-rich strata in the Ferris Formation. These outcrops lie along the flanks of Simpson Ridge anticline, along Number 5 Ridge (Fig. 2). Compared to other Ferris Formation outcrops, concretions are abundant, large, and well-exposed. These dark masses are developed in light-colored, 1–2-m-thick bodies of fine, structureless to faintly cross-bedded sandstone (Fig. 4A). The sandstones are tabular and show few signs of channeling. We found neither body fossils nor trace fossils in the concretion-bearing rocks.

In strongly weathered outcrops, disintegrating concretions are defined by piles of centimeter-scale, angular blocks of iron-oxide-cemented sandstone. In road cuts and in some natural exposures, the concretions are seen to be ovoid to tabular and up to 1 m thick and 3 m long (Fig. 4). Macroscopically, iron-oxide cement forms: 1) single or multiple, isopachous rinds from 3 mm to 1.0 cm thick that envelop many of the concretions; and 2) isopachous linings of rock fractures that are present in the concretions (Fig. 4B). The iron content of sandstone in the concretions diminishes inward from edges of blocks defined by the rinds and joints. Thin sections show that all iron is present as iron oxide; we did not observe

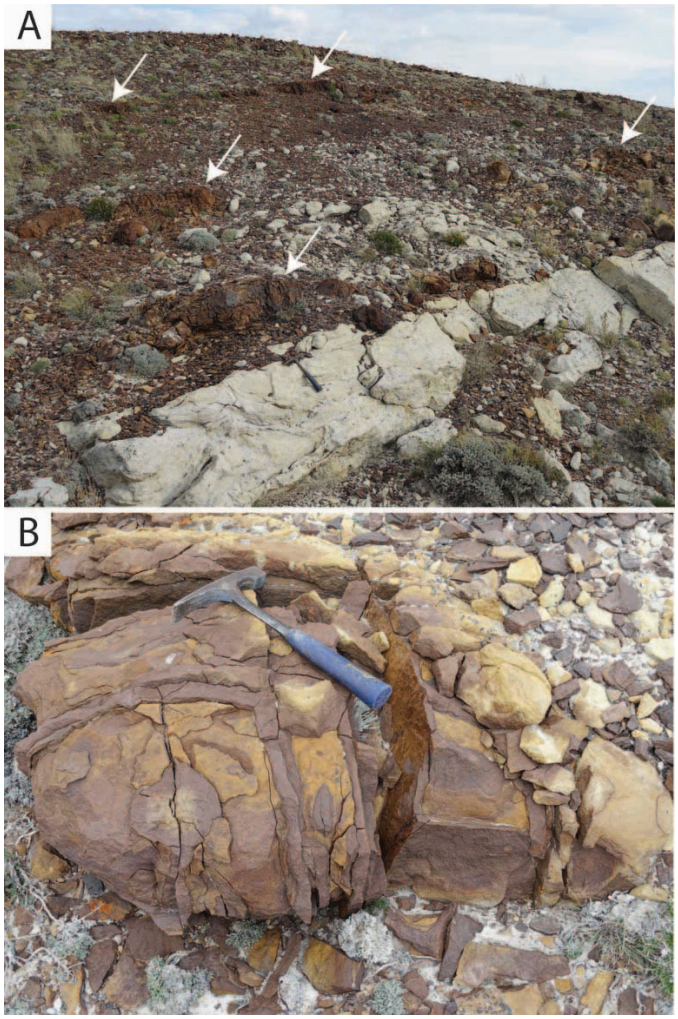

FIG. 4.—*In situ* iron-oxide-cemented concretions in sandstone, Ridge No. 5; see Figure 2 for location. **A)** Ovoid to tabular iron-rich masses (arrows) originally grew as siderite concretions within a matrix of light-colored, tabular sandstone. **B)** Ovoid concretion with multiple fractures lined by iron-oxide-cemented sandstone. Fractures provided conduits for O_2-rich water during siderite oxidation. Longest axis (left-right) and intermediate axis (top to bottom of photo) of the concretion grew parallel to bedding of the host sandstone.

siderite. In the concretions, iron oxide occurs as intergranular cement in a grain-supported sandstone matrix. Thin sections show very few grain-to-grain contacts; cement and primary pores occupy 45–50% of the rock fabric. In rinds and fracture linings of the concretions, pores are completely filled by cement (Fig. 5A); in the inner portions of concretions, primary pores are surrounded by meniscate, iron-oxide cement (Fig. 5B). Iron-oxide cement immediately adjacent to the meniscate cements commonly forms small (~ 0.1 mm) rhombs (Fig. 5B). In hand specimens, the inner portions of some concretions have a speckled appearance; a hand lens reveals these speckles to be millimeter-scale, irregular- to rhomb-shaped, masses. Thin sections show that each mass contains numerous detrital grains (Fig. 5C, D).

Interpretation

Even though siderite is absent from the outcrops of the study area, a sideritic origin for the concretions is supported by our field observations and thin sections. Siderite is a common mineral in sedimentary rocks, but it is stable only in reducing pore waters (Berner 1971). It is absent in the concretions that crop out in our study area because these concretions formed in porous and permeable rocks. From *in situ* concretions in Triassic and Jurassic strata, Loope et al. (2010, 2011), Loope and Kettler (2015), and Burgess et al. (2016) described morphologic features very similar to those seen in the concretions of our study area, and attributed them to siderite oxidation.

Primary (*de novo*) iron oxide accumulations are difficult to explain. In waters with nearly neutral pH, iron is soluble only in reducing environments as Fe^{++}. These waters instead precipitate ferrous minerals like siderite, pyrite, and marcasite. According to Curtis and Coleman (1986), most iron-oxide concretions are best interpreted as the oxidized remains of reduced-iron precursors. Rinds formed along concretion perimeters and along internal fractures below the water table where reactions were likely catalyzed by iron-oxidizing microbes that occupied redox boundaries between diffusing oxygen and diffusing ferrous iron (Weber et al. 2012). Rhomb-shaped masses and meniscate iron-oxide cements (Fig. 5B) formed in the vadose zone (see Loope and Kettler 2015). We interpret the rhombic masses of iron oxide as pseudomorphs after euhedral siderite (Fig. 5A, D). The larger rhombic to irregular "speckles" (Fig. 5C, D) are composed of iron oxide that replaced poikilotopic siderite crystals. Preservation of pseudomorphs required *in situ* oxidation of the euhedral siderite crystals—ferrous iron did not diffuse along centimeter-scale paths as it did during rind formation.

The large size, ovoid shape, and uncompacted fabric of the Ferris concretions are similar to those described by Gautier (1982) from outcrops and cores of the Cretaceous Gammon Shale (marine; northwestern Wyoming and western South Dakota). The large fraction of pore-filling cement in the Ferris Formation (Fig. 5A) indicates that the siderite concretions formed early (pre-compaction). Post-depositional uplift, denudation, and fracturing of the Ferris and Hanna formations allowed oxygenated meteoric water to infiltrate the porous sandstone and its concretions, leading to alteration of the siderite to iron oxide.

The abundance of coal, the relative scarcity of pyrite, and the evidence of an abundance of siderite cement in the Ferris Formation all suggest a nonmarine setting for the strata of our study area. However, recent detailed studies of sedimentary structures in some Ferris Formation sandstones suggest at least the episodic presence of shallow marine conditions during Ferris deposition (Boyd and Lillegraven 2011). We interpret the tabular sandstones in the study area as meandering-stream deposits. Deciphering the position of the paleo-shoreline is difficult. The presence of the large and abundant siderite concretions suggests that the sulfate concentration in the pore water was low during early diagenesis—an indication that the concretions did not form in marine pore water (Berner 1981; but see Gautier 1982). In our study area, Wroblewski (2006) reported evidence for marine conditions in the form of sedimentary structures indicative of tidal deposition that contained the skeletal remains of selachian fishes above the Hanna–Ferris contact and interpreted those deposits as estuarine. The ichnogenus *Rhizocorallium* is widely recognized as originating in marine, subtidal environments and has been found in abundance in the uppermost third of the Ferris Formation in an outcrop about 45 km WNW of our study area. Boyd and Lillegraven (2011) argued that the Hanna basin was episodically connected to either the Cannonball Seaway or a Gulf Coast embayment. Because we have not recognized body fossils or trace fossils indicative of marine conditions, we favor a nonmarine coastal plain as the depositional setting for the Ferris Formation sandstones that host the large concretions.

REWORKED, IRON-RICH CONCRETIONS

Description

Reworked, iron-rich concretionary clasts are prominent components of conglomerates near the base of the Hanna Formation and lie south and

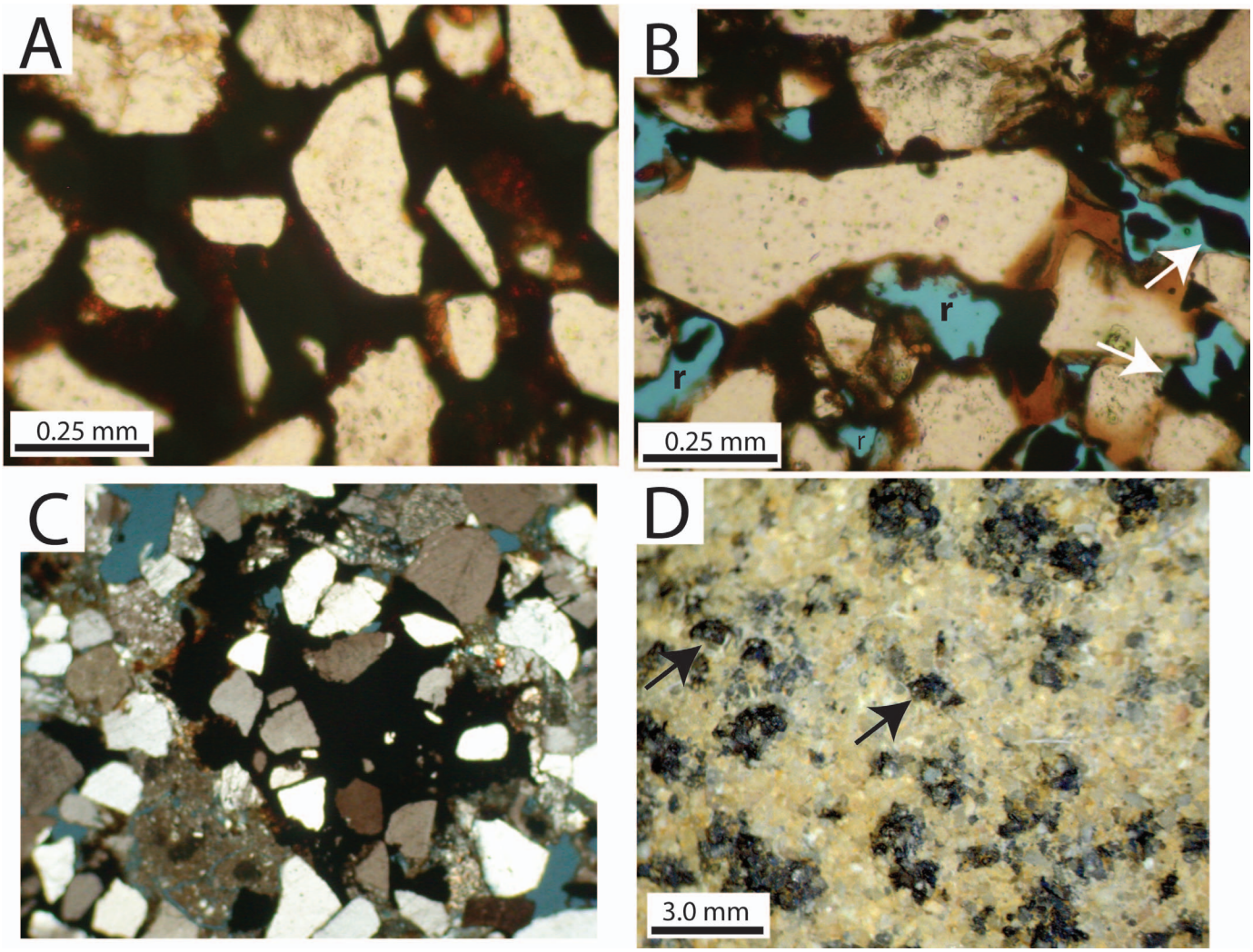

FIG. 5.—*In situ* concretions: photomicrographs (A, B, C) and close-up of speckled hand specimen (D). **A)** Dense iron-oxide-cemented rind, plane light. Note open fabric with few grain contacts. **B)** Central portion of iron-rich concretion with meniscate, iron-oxide cement and rounded pores (r), filled with blue epoxy (plane-polarized light). Arrows point to iron-oxide rhombs, interpreted as pseudomorphs after siderite that were oxidized in the vadose zone. **C)** "Speckle" of iron oxide cement that encloses numerous quartz grains (crossed-polarized light). D) Close-up photo of hand specimen of the speckled center of a concretion. Arrows point to rhombic speckles.

southeast of Ferris Formation outcrops containing abundant *in situ* concretions (Fig. 2). These conglomerates are best exposed at Grayson Ridge and Halfway Hill (Figs. 2, 6) where they underlie well-sorted sandstones. Soft-sediment deformation is present in both the sandstones and the conglomerates of the lower Hanna Formation (Figs. 6–8). In addition to the reworked, iron-rich concretions in the conglomeratic strata, the sandstones contain large, *in situ*, concretions cemented by ferroan calcite. At the study site west of Carbon, many of these concretions are pipe-like in form and are aligned SSE (Fig. 9; $\chi = 157°$; $\sigma = 8.2°$; $n = 18$). Crossbedded sandstones—the matrix for the pipes—have foresets that dip in the same direction (Figs. 2, 10).

Reworked, concretionary clasts range in diameter from < 1 cm to > 2 m. Rinds composed of iron-oxide-cemented sandstone are especially prominent on relatively small, discoidal clasts that comprise grain-supported, well-sorted conglomerates and form lags at the bases of many sandstone bodies (Fig. 11A, B). In weathered cross sections, many of these smaller clasts are hollowed out—their friable interiors have fallen away, leaving shell-like rinds and internal fractures lined on both sides by iron-oxide cement (Fig. 11A). Some of the larger reworked clasts are also rinded, but their rinds are typically incomplete (Fig. 11D). The large clasts are cut by numerous orthogonal fractures, many of which are lined by iron oxide. Haloes of angular, iron-rich, blocky fragments surround some of the large, reworked clasts (Fig. 11D), and similar, small blocky fragments are also common constituents of conglomerates (Fig. 11C). Large, tabular fragments of stratified, highly friable, iron-poor sandstone and siltstone are also present in some poorly sorted conglomerates (Fig. 12). The largest reworked, iron-rich concretionary clast (1 m $\times$ 1 m $\times$ 2 m) rests upon conglomerate marking an intraformational Hanna unconformity (Fig. 6; Secord 1998, 2006), but is surrounded and overlain by bedded, well-sorted sandstone (Fig. 7). This lag deposit lies just above a thick sandstone with over-steepened, contorted bedding (Fig. 7B). At a slightly lower stratigraphic level below the intraformational unconformity, numerous large concretionary clasts are present in a structureless, sandy matrix (Figs. 6, 8).

Interpretation

Reworked, iron-rich concretions in the Hanna Formation conglomerates were derived from nearby, *in situ,* iron-rich concretions in the Ferris Formation. Iron-oxide-cemented rinds and joint linings present in both *in*

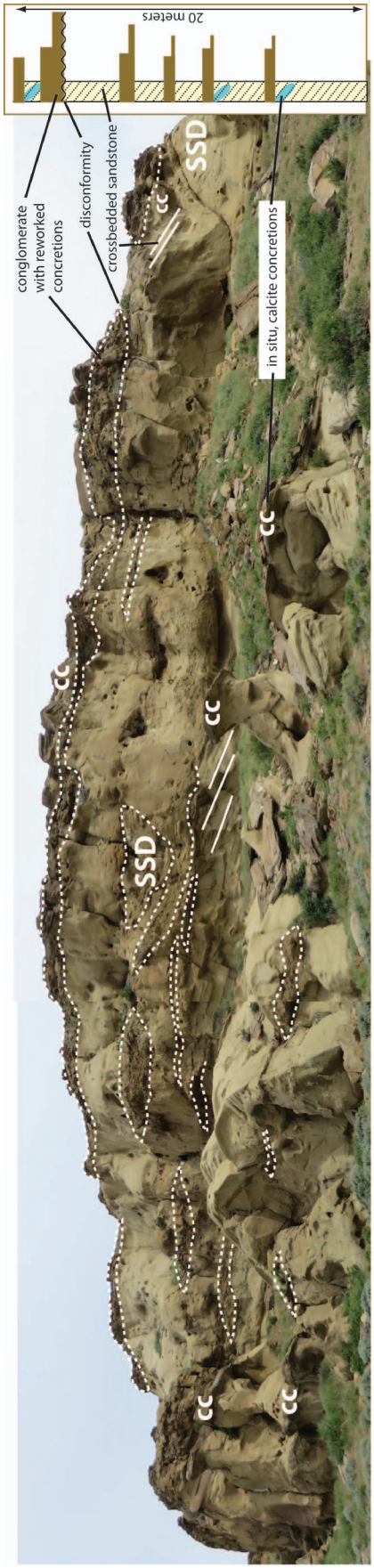

FIG. 6.—Southeastern portion of the valley fill at the base of the Hanna Formation exposed at Halfway Hill (viewed from the south). Height of outcrop is 20 meters. Dashed lines surround conglomeratic beds; the conglomerate near top of exposure rests on an intraformational (Hanna) unconformity. All conglomerates contain reworked, iron-oxide-cemented concretions. Straight lines are parallel to large-scale crossbeds. SSD marks soft-sediment deformation, and CC marks calcite concretions.

situ and reworked concretions indicate that all are the oxidized remains of siderite-cemented concretions. The smaller, discoidal clasts with isopachous rinds (Fig. 11A) are similar to the reworked concretions in the Dakota Formation of eastern Nebraska (Loope et al. 2012) and to similar masses in Pleistocene alluvium of the Netherlands (van der Burg 1969). These clasts were reworked and rounded while still siderite-cemented—their complete (unabraded) rinds formed after transport and deposition when the internal siderite dissolved and the diffusing ferrous iron was oxidized at clast perimeters. These clasts were likely derived from *in situ* concretions that had encountered neither oxidizing groundwater nor the vadose zone. Many of the larger clasts, however, show evidence of oxidation, both above and below the water table, before transport. Unlike the smaller clasts, rinds on the larger clasts are commonly incomplete, indicating that they formed in oxidizing groundwater before transport and were abraded and partially lost during transport. Dispersed, blocky, centimeter-scale iron-rich clasts (Fig. 11C) represent the scattered remains of large, oxidized concretions that did not survive transport. Haloes composed of similar angular, blocky fragments that surround some large clasts (Fig. 11D) indicate that at least some of the large, already thoroughly-oxidized clasts did, however, survive transport.

The large sizes of many of the clasts suggest transport along the relatively steep surfaces of alluvial fans rather than by low-gradient rivers (see Blair and McPherson 1994). Although it is possible that these clasts were transported to trunk streams by sediment gravity flows, none of the preserved (and exposed) strata reflect deposition via these processes. We interpret the preserved deposits that contain the large clasts as winnowed lags that formed in river channels.

Soft-sediment deformation is the best explanation for large concretionary clasts "floating" in structureless sandstone (Fig. 8). Large, dense (iron-rich) clasts in well-stratified lags descended into sand that was liquefied during seismic events equal to or greater than M5 (Ambraseys and Sarma 1969). These deformation structures are fully consistent with a syntectonic interpretation (see Aschoff and Schmitt 2008).

We have seen no evidence of reworking of the ferroan-calcite-cemented concretions (Figs. 1, 9, 10B). Bedding can be traced from concretion interiors into the surrounding sandstone. These concretions formed in highly permeable, well-sorted sands. During their growth, pore waters were reducing, but calcium ions were much more abundant than ferrous iron. Ferroan calcite remains unoxidized because it contains much less ferrous iron than siderite; lithautotrophic, iron-oxidizing microbes cannot metabolize carbonate minerals with less than 50 mole% Fe (see Loope et al. 2010, p. 1002). Schultz (1941) was the first to note that pipe-like concretions form parallel to the direction of groundwater flow; subsequent studies have confirmed this relationship (Mozley and Davis 1996; Cavazza et al. 2009). The SSE alignment of the pipe-like concretions west of Carbon is parallel to the dip direction of crossbeds from the same area (Figs. 2, 8).

We did not investigate the provenance of the friable sandstone clasts in the Hanna Formation (Fig. 12). We speculate that they may represent fragments of the sandstone matrix of the Ferris concretions.

SOURCE AREAS, TRANSPORT DIRECTIONS, AND SEDIMENTARY PROCESSES

Description

Paleocurrent directions based on crossbeds in the Hanna and Ferris formations in the Hanna and Carbon basins were reported by Ryan (1977), Secord (1996), and Wroblewski (2003, 2006). Secord (1996) took measurements on trough crossbeds from the principal areas where the iron concretions are abundant. Resulting paleocurrent vectors (calculated with "Rockware" software) are shown on Figure 1; rose diagrams and statistics are given in the supplemental file (Fig. A1, see Supplemental Material). Our measurements indicate bimodal flow in the Ferris

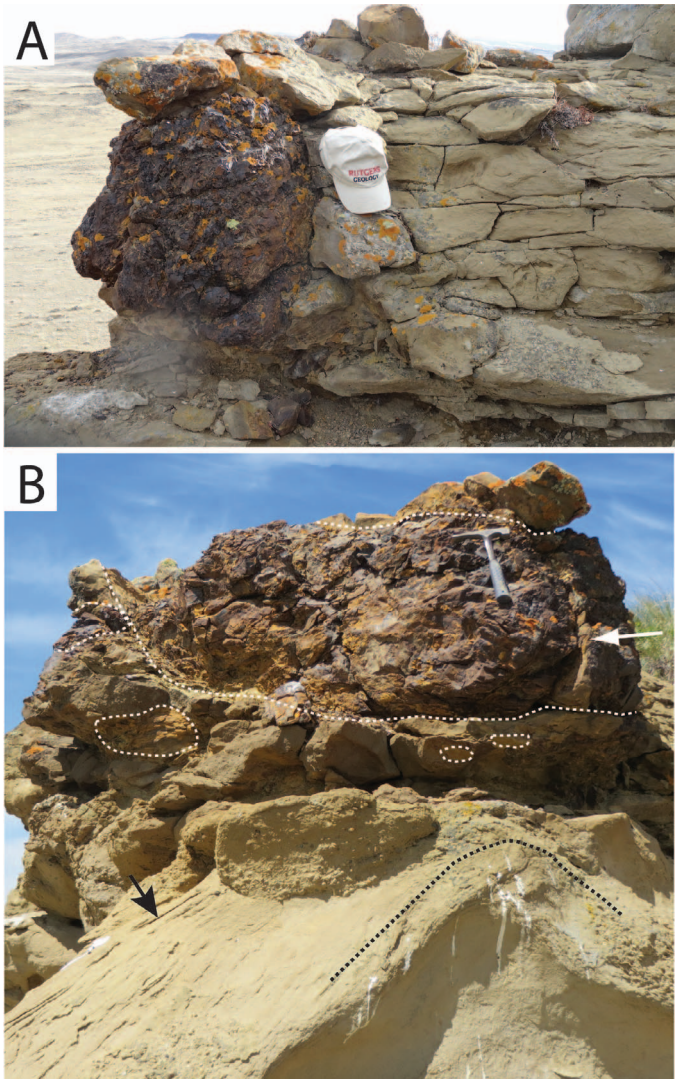

FIG. 7.—Largest observed concretionary clast in a lag deposit marking intraformational Hanna unconformity, crest of Halfway Hill (41°48.88′N; 106°15.70′W). **A)** In view from the east, clast is surrounded and overlain by bedded sandstone. **B)** Viewed from south, the clast rests on other reworked clasts (outlined in white). Sand-filled crack in largest clast (white arrow) and sandstone with oversteepened and folded bedding (black arrow and black dashed line) are interpreted as products of earthquake-induced fluidization and liquefaction.

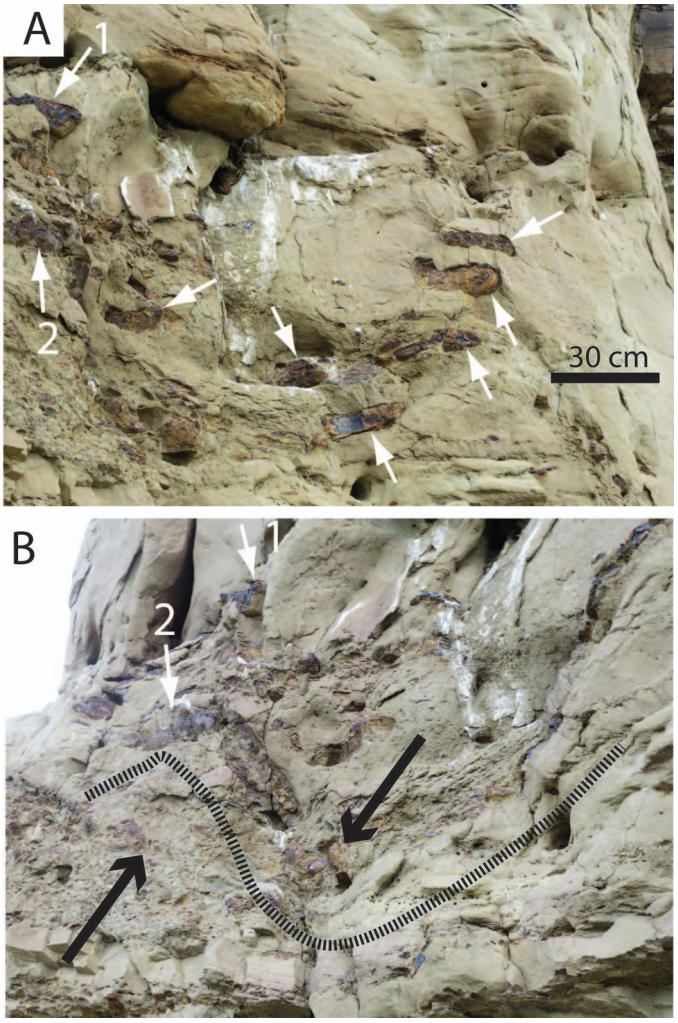

FIG. 8.—Iron-rich clasts in the Hanna Formation. Conglomerate on south-facing cliff at Halfway Hill. **A)** Large clasts (arrows) "float" in structureless sandstone matrix. **B)** View of same outcrop from a different angle suggests that the matrix-supported fabric was produced by soft-sediment deformation. Dashed line is interpreted as a contorted bedding plane.

Formation, with southwestward and southeastward components at Grayson Ridge (the only place with reworked conglomerates in the Hanna where multiple measurements can be made on the underlying Ferris). Vector analysis indicates that the southwestward component was the strongest (Fig. A1). In contrast, all vectors calculated for the Hanna Formation indicate predominant southeasterward flow suggesting a change in paleocurrent directions from southwestward in the Ferris Formation to southeastward in the Hanna Formation. Our paleocurrent directions in the Hanna Formation are in good agreement with previous studies, two studies (Ryan 1977; Wroblewski 2006) reported stronger southeastward flow in the Ferris Formation.

For the Hanna Formation in the Hanna basin, Ryan (1977) showed that pebble sizes and feldspar frequency indicate a northern source of sediment. On the basis of petrographic evidence, he found no compelling evidence for movement of sand across the anticline into the Carbon basin. He concluded that the Simpson Ridge anticline was active during deposition of the Ferris and Hanna, forming a nearly complete sedimentation barrier between the two basins. Compared to the Ferris Formation, the Hanna Formation records a later pulse of coarser sediment with higher aggradation rates (Ryan 1977).

Interpretations

We agree with Wroblewski (2003): the Ferris and Hanna formations are syntectonic, and record the ups and downs of the Simpson Ridge anticline. Here, the rocks comprise growth strata (Suppe et al. 1992); their deposits are analogous to those that surround the actively rising and laterally propagating Wheeler Ridge anticline in the southern San Joaquin Valley of California (Burbank et al. 1996; Keller et al. 1998). The Wyoming strata were deposited by aggrading, antecedent rivers that flowed across an actively deforming anticline (Fig. 3). Sections of the lower Hanna Formation containing reworked concretions (Fig. 6) record an episode when aggradation across the crest of the structure ceased and erosion by antecedent rivers dominated.

Ryan's (1977) and Wroblewski's (2003) paleocurrent data from Ferris Formation outcrops in the southeastern part of the Hanna basin (along the

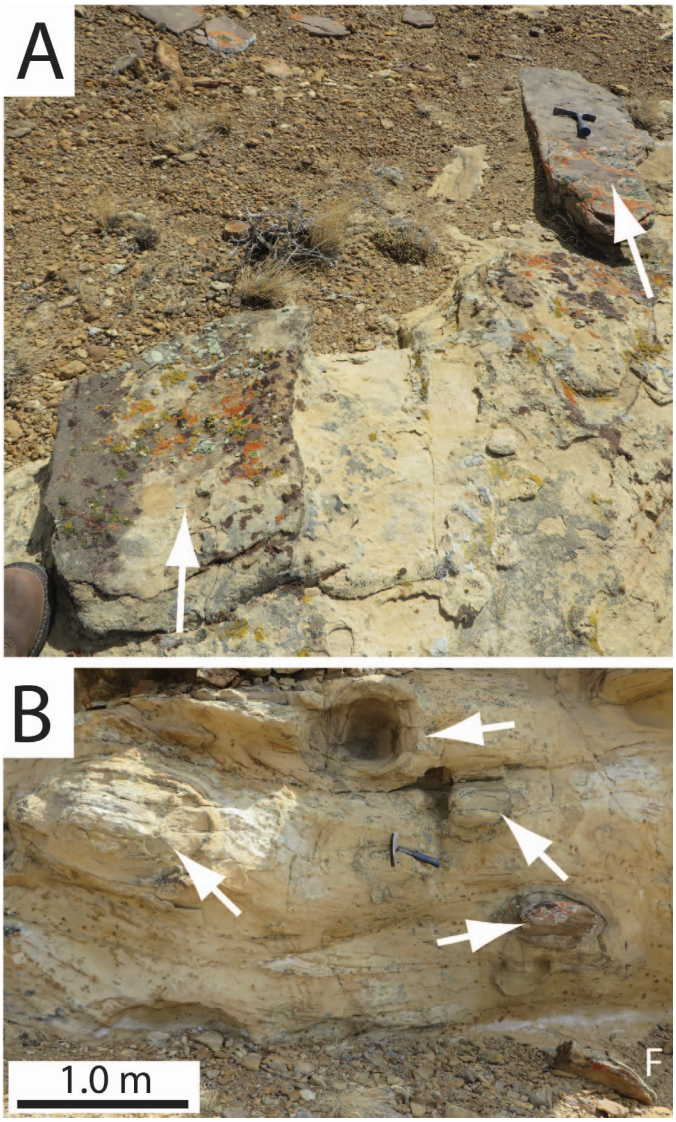

FIG. 9.—Pipe-like concretions west of Carbon (Fig. 2). **A)** Incomplete, lower portions of two *in situ* concretions oriented S30°E. **B)** Cross-sectional view of pipe-like concretions. Rock at "F" is a fallen fragment of the *in situ* pipe above it.

western edge of the Simpson Ridge anticline) show transport to the northeast; those at the nose of the anticline show transport to the east (Fig. 2). Both workers interpreted these data as evidence for diversion of the Ferris drainage pattern along the strike of the anticline and around its nose. Both concluded that the Hanna and Carbon basins became two separate basins during Ferris and Hanna deposition, with only a narrow connection (for both formations) at the nose of the Simpson Ridge anticline. Some of Ryan's data for Hanna Formation crossbeds in the southeastern Hanna basin and at the western margin of the Carbon basin, however, show an eastward vector as much as 13 km south of the anticlinal nose; Secord's (1996) data also reflect this eastward vector (Fig. 2). These data help to confirm that, in our study area, both formations were deposited by an antecedent river system.

Geomorphological studies of active tectonic folding in the San Joaquin Valley (Keller et al. 1998; Talling and Sowter 1999) show that some antecedent streams that flowed perpendicular to the rising structures were able to maintain their positions, producing water gaps; other antecedent streams were eventually diverted laterally around the structures, leaving wind gaps. In their study of the Zagros Mountains of southern Iran, Ramsey et al. (2008) showed that the stream patterns between rising anticlinal folds provide evidence that the folds there are propagating laterally and "pinching" streams between fold tips. Burbank et al. (1996) summarize the many different geologic and geographic factors that determine whether transverse, antecedent streams can maintain the courses across rising structures or are, instead, deflected.

We argue here that the large concretionary clasts in the Hanna Formation were derived from *in situ* concretions in the Ferris Formation and that these clasts were carried down the slopes of the rising Simpson Ridge anticline and, perhaps, over small alluvial fans built into the Carbon basin (Fig. 2). Our data agree with Ryan's (1977) and Wroblewski's (2003) interpretations (for both the Ferris and Hanna) relating to the anticlinal nose but disagree with Ryan's (1977) view that the two basins remained separate. Ryan's (1977) data, together with Secord's (1996) and our data, indicate that, for the Hanna Formation of the Carbon basin, southeast-flowing, antecedent rivers crossed the rising anticline in a swath at least 5 km wide and deposited reworked concretions (Fig. 2) across its axis at least 7 km south of the anticlinal nose.

Siderite concretions commonly precipitate in reducing groundwater where microbes metabolize dissolved organic matter and methane. A thin package of flat-lying strata deposited by antecedent rivers that drain a coal basin (like the Hanna basin) and flow over the crest of an anticline is chemically and physically favorable for nucleation and growth of siderite concretions (Fig. 3). Mozley et al. (1995) and Hall et al. (2004) showed that calcite concretions in fluvial deposits in the Santa Fe Group (Oligocene–Pleistocene, central New Mexico) preferentially grew in strata with the greatest pre-cementation porosity. They attributed this to the greater flux of calcium and bicarbonate ions through the most permeable part of the aquifer. We note that, due to the impermeability of the underlying Medicine Bow Formation and Lewis Shale, groundwater in the sandy Ferris–Hanna aquifer was forced to accelerate as it moved through the thinning wedge of growth strata (Fig. 3; Freeze and Cherry 1979, p. 21). In the subsurface, groundwater flow paralleled stream flow—west to east from the Hanna basin into the Carbon basin (Fig. 3). By increasing the flux of calcium, ferrous iron, and bicarbonate ions, and of dissolved organic matter, vertical and lateral convergence of the groundwater flow system likely played an important role in the growth of the large siderite concretions in the Ferris Formation, and in the later growth of the large ferroan calcite concretions in the basal Hanna Formation.

Large concretions in the basal Hanna Formation—eroded from uplifted Ferris Formation—were likely transported to the trunk stream by slumps and small alluvial fans; these large clasts are now preserved as lags that are interbedded with crossbedded sandstone. Due to the generally non-resistant character of the rising strata, we doubt that large fans developed on the flanks of the Simpson Ridge anticline. A modern analog, Wheeler Ridge, stands 300 m above the San Joaquin Basin, but the fans on its north (distal) flank have built only $\sim$ 1 km into the adjacent basin.

By far the thickest and most numerous conglomeratic beds as well as the largest reworked concretionary clasts of the basal Hanna Formation in the Carbon basin lie along the axis of the Halfway Hill syncline. We consider this an example of preferential preservation: the conglomeratic strata along the axis of the syncline (Fig. 6) were protected from post-tectonic erosion. Because we also observed reworked concretions west of Carbon (well south of the Halfway Hill syncline, Fig. 2), we think the antecedent river eroded a wide swath across the anticline, not a narrow paleovalley. The thick, well-sorted, SSE-dipping crossbeds with SSE-oriented pipe-like concretions in the Hanna Formation cropping out very near the axis of the Simpson Ridge anticline (west of Carbon; Fig. 2) indicate that the lower Hanna Formation was deposited by a SSE-flowing, antecedent river. After an episode of sediment bypass, aggradation started to again outpace the upward propagation of the growing anticline (Burbank et al 1996), and

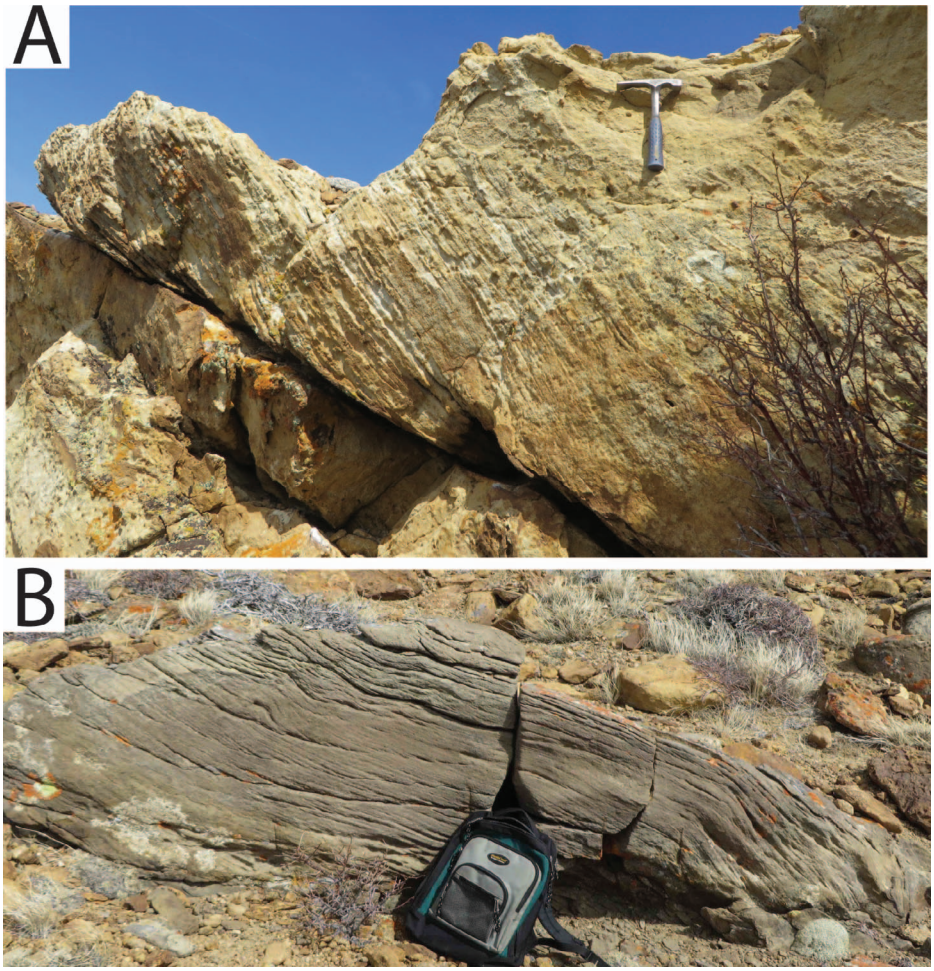

FIG. 10.—Hanna Formation crossbeds, west of Carbon (see Fig. 2 for location). **A)** Southeast-dipping crossbeds near base of the Hanna Formation (41° 50.9076′ N; 106° 23.8434′ W). **B)** Portion of a calcite-cemented concretion that grew within and enclosed deformed crossbeds.

spread a broad, continuous sheet of sandy sediment that spanned the Hanna and Carbon basins.

DISCUSSION

Recognition of reworked concretions helps to constrain the timing of concretion growth. Confusing a reworked concretion with an *in situ* concretion (or ignoring all concretions) results in the loss of important provenance information. If well exposed, concretions that occur in conglomeratic strata with grain-supported fabrics are easy to recognize as reworked clasts (Fig. 9A–C; Table 1). Isolated concretions in a structureless matrix are more difficult to interpret. The texture and fabric of clasts in *in situ* concretions closely resemble those of the hosting clastic sediment. The texture and fabric of detrital clasts in a reworked concretion, however, are likely to differ substantially from the texture and fabric of the hosting matrix (Table 1). Reworked concretionary clasts are much more likely to be actively involved in soft-sediment deformation (Fig. 8) than are *in situ* concretions, but *in situ*, late diagenetic concretions can passively grow to enclose soft-deformation structures in well-sorted sandstones (Fig. 10B).

Although they can provide key evidence for syntectonic erosion and deposition, reworked, iron-rich concretions do not, by themselves, necessitate uplift or unconformable relationships. Reworked, sideritic concretions are common in the deposits of post-Silurian meandering fluvial systems, where migrating channels erode marshy or forested floodplain deposits. Rinded concretions (the oxidized remains of early-diagenetic, sideritic mudballs) are common in both the Triassic Shinarump Member of the Chinle Formation (northern Arizona; Burgess et al. 2016) and the Dakota Formation (eastern Nebraska; Loope et al. 2012). Reworked, very young, iron-rich concretions can also be found on marine sand flats and tidal creek beds (Pye et al. 1990). The stark differences, however, between the fine-grained sandstones that host *in situ* concretions of the Ferris Formation (Fig. 4) and the conglomeratic and large-scale crossbedded strata that host the reworked concretions in the Hanna Formation indicate that reworking of the concretions was not an autocyclic process that operated in a single depositional setting.

The permeability of hosting strata determines the diagenetic fate of siderite concretions. The large-scale, internal structure of the concretions described here—the enveloping rinds and fracture linings—are very similar to those in concretions of the Jurassic Navajo Sandstone (eolian; southern Utah). Like the concretions described here, those in the Navajo also contain abundant iron-oxide pseudomorphs after euhedral, rhombic siderite crystals (Loope et al. 2011; Loope and Kettler 2015). In contrast, outcrops of the Cretaceous Gammon Shale (Gautier 1982), which are now exposed to climate and vegetation that are similar to those in our study area, contain abundant siderite and very little iron oxide (Fig. 13; Gautier 1982). The carbon-rich, low-permeability host rocks apparently prevented oxygenated water from reaching and penetrating the Gammon concretions.

The lithology and location of the very large, reworked, iron-rich concretions in the Hanna Formation of our study area—found at Grayson Ridge and Halfway Hill (Fig. 2)—indicate that, during middle Paleocene tectonism, many Ferris Formation concretions were fractured and uplifted into the vadose zone before they were entrained, transported, and deposited. Because of their size and relative fragility, we consider it unlikely that the

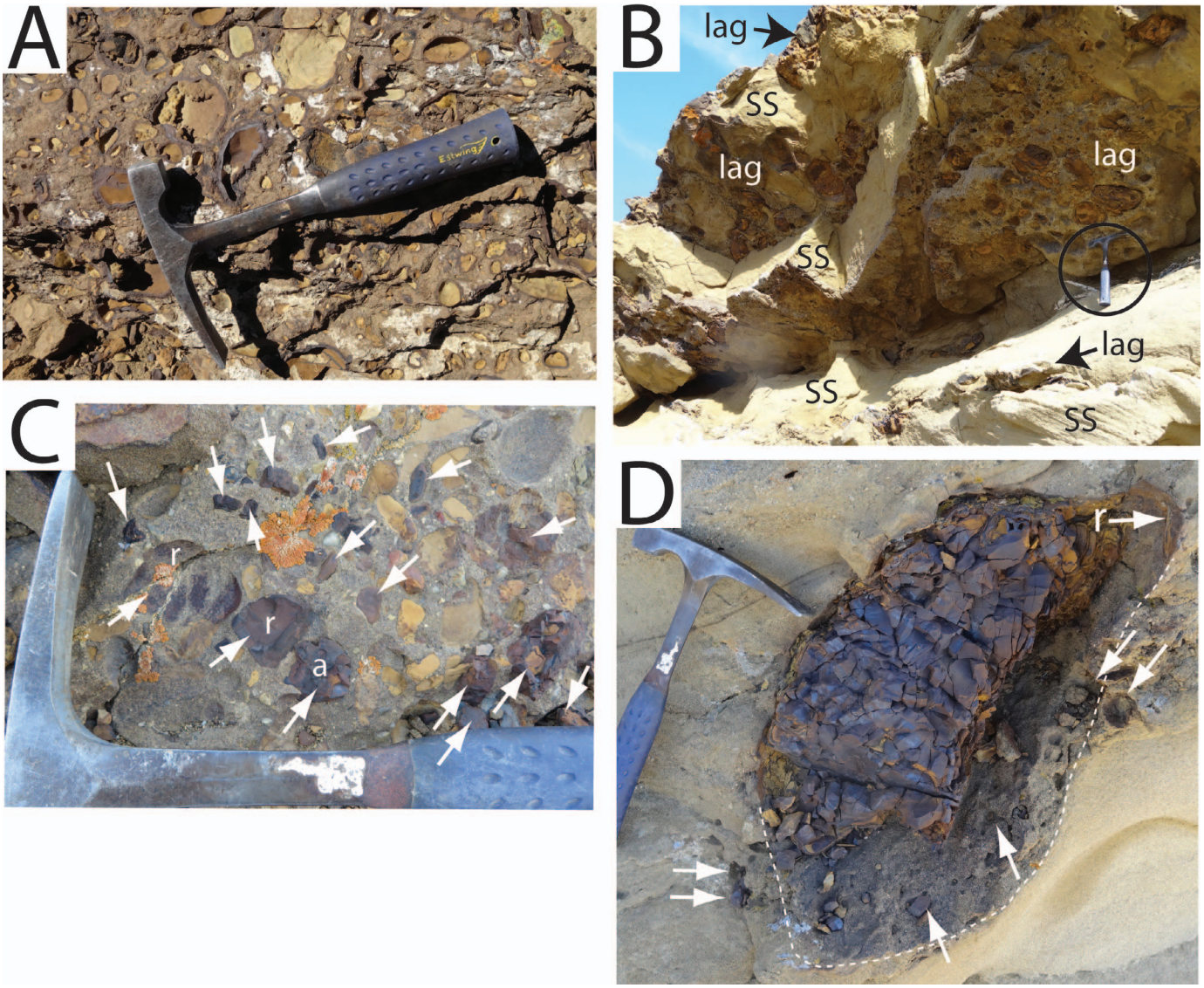

FIG. 11.—Reworked concretionary clasts (Hanna Formation). **A)** Small clasts in a well-sorted, clast-supported conglomerate. Note entire, iron-oxide-cemented rinds on each clast (Halfway Hill). **B)** Four conglomeratic lags composed of concretionary clasts; each is underlain by a bed of well-sorted sandstone (SS). Hammer is circled. **C)** Small, angular (a) and rounded (r), iron-rich clasts. **D)** Large, isolated, highly fractured clast with a partial rind; the clast is surrounded by a halo of angular, iron-rich fragments. The interpretation is that small clasts in the Hanna Formation (Part C) were derived from large concretions that were oxidized and fractured during subaerial exposure of the Ferris Formation; some of the large clasts in the Hanna (Part D) were carried away from Ferris outcrops by mass wasting or stream floods before their breakup into smaller clasts.

concretions exposed near the top of the section at Halfway Hill (Figs. 6, 7) were transported 13 km from the nose of the Simpson Ridge anticline. The Ferris–Hanna contact is exposed in only a small portion of the Grayson Ridge exposure, so there is little direct evidence available to constrain their precise provenance. We consider it most likely, however, that some of the large concretions at the base of the 20-m-thick section at Halfway Hill (Fig. 6) were exhumed in the bed of the antecedent river immediately upstream where the river was cutting through the concretion-bearing portion of the Ferris Formation. The majority of the concretions (those higher in the section) were likely delivered to the trunk stream by gullies and small-scale alluvial fans or (directly) by mass wasting of the paleovalley walls when downcutting ceased and the valley began to fill.

Although the tectonic (klippe) hypothesis (Lillegraven 2015) cannot be entirely refuted, it is far less parsimonious than the source–sink (autochthonous) argument that we advance here in which large, reworked concretions in the basal Hanna Formation of the Carbon basin are explained by erosion of *in situ* concretions in directly subjacent and proximal Ferris Formation strata. Lillegraven (2015) reported that the contact between the Hanna Formation and underlying rock units was tectonic everywhere it could be observed. The Hanna–Ferris contact, however, is poorly exposed in most of the Carbon basin. Grayson Ridge is the only place we observed where the contact is fairly well exposed, but we found no evidence there that the contact is structural. The kinds of evidence (e.g., faulting, folding, fault gouge) that would be expected along a contact in which a massive body of rock had been moved $>$ 10 km appear (to us) to be absent.

The Hanna basin and surrounding Laramide block uplifts in south-central Wyoming may have played important roles in the routing of a major middle Paleocene to early Eocene river system that originated in southern California and Idaho and debouched into the Gulf of Mexico during

FIG. 12.—Conglomerate (Hanna Formation) at Grayson Ridge (below intraformational unconformity) composed of iron-rich concretionary clasts (white arrows) and very friable, imbricated sandstone clasts (black outlines).

deposition of the lower Wilcox Group (Blum and Plecha 2014; Sharman et al. 2017). The conglomeratic Paleocene fluvial strata in the Carbon basin described here could have been deposited by rivers originating in California. Our work suggests a larger (5-km-wide) river system evolved from the several narrow paleovalleys envisioned by Wroblewski (2006). Sharman et al. (2017) recognized that the hiatus that developed in the lower Hanna Formation (Secord 1998, 2006) could very well represent an episode when sediment, rather than being trapped in a Laramide basin, bypassed to downstream basins.

CONCLUSIONS

If early diagenetic concretions form in the deposits of streams that cross rising anticlines, they are likely to be reworked when aggradation is

TABLE 1.—*Characteristics of* in situ *and reworked concretions*.

	In Situ	Reworked
Relation to host beds (outcrop)	-Long and intermediate axes oriented parallel to bedding (including crossbeds) -Spheroidal if in structureless matrix -Nucleated along a few preferred bedding planes -Commonly appear in deformed beds if late diagenetic	-Long and intermediate axes commonly at high angles to bedding; if platter-shaped, can be imbricated -Usually accompanied by other coarse clasts in grain-supported lag, but also occur as isolated clasts in finer-grained matrix (as clasts in a debris flow, or as result of mixing during soft-sediment deformation)
Texture and fabric (microscope)	-Grain size same as host; can show bedding. -Fabric may be "exploded" due to force of crystallization.	-Grain size differs dramatically from hosting matrix (i.e., mudstone-based concretion in sandy to conglomeratic host beds -Orientations of long axes of grains differs from those in host beds

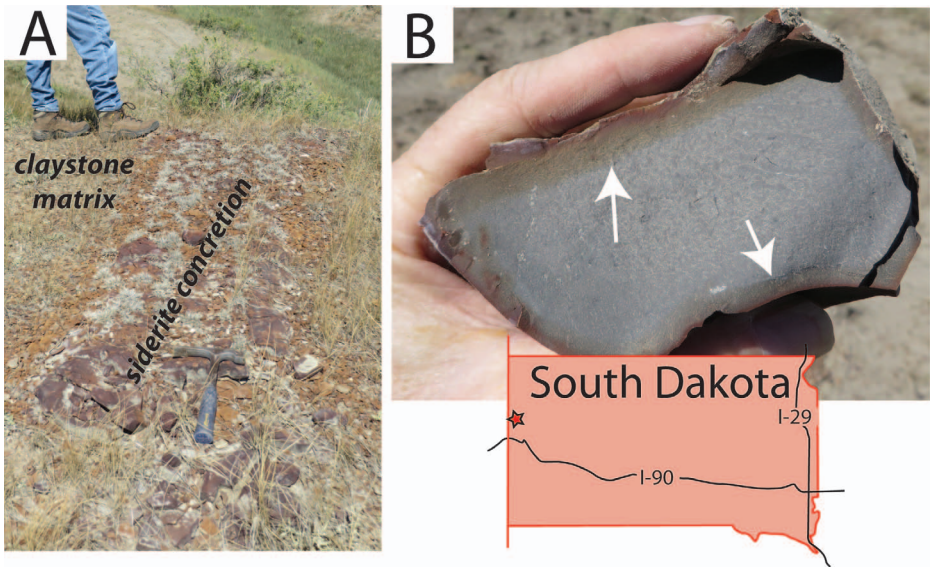

FIG. 13.—Fully preserved, *in situ* siderite concretions in the Upper Cretaceous Gammon Shale, western South Dakota (see Gautier 1982, Lower Owl Creek locality, p. 862). **A)** Large concretion exposed on ridge crest. **B)** Freshly broken concretion in which micritic siderite is only superficially oxidized; arrows point to inner edge of the lightly oxided zone.

followed by erosion during fold growth. If reworked concretions are confused with *in situ* concretions or if concretions are ignored, important provenance information is lost. Generally, poor cementation of aggrading sediment leads to persistence of antecedent streams (Burbank et al. 1996). Concretion growth can leave the bulk of the host sediment uncemented and easily erodible, but, with time, could lead to assembly of a resistant, armored surface that could bring about the defeat and diversion of the stream.

The coarse, concretionary debris in the basal Hanna Formation in our study area was derived from *in situ* concretions in the Ferris Formation while the Ferris was being actively deformed along the axis of the Simpson Ridge anticline. The diagenetic and transport history of the iron-rich concretions reflects the evolving interaction of tectonic, fluvial, and geochemical processes: 1) As Simpson Ridge rose beneath rapidly aggrading, permeable sands, the ionic composition and high flux rate of reducing groundwater allowed large siderite concretions to grow in the Ferris Formation. 2) When aggradation slowed or the uplift rate increased, concretions entered shallow, oxidizing groundwater. Microbes built dense iron-oxide rinds along internal fractures and on the perimeters of most concretion as siderite dissolved and ferrous iron started to diffuse throughout the water-saturated concretions. 3) When concretions rose into the vadose zone, remaining siderite crystals were oxidized *in situ*. 4) Eroded concretionary material was transported southeastward and deposited (into the basal Hanna Formation) by a southeast-flowing river. 5) Downcutting through Ferris Formation strata that contained the largest concretions was followed by mass wasting of valley or gully walls and fan-building by short tributaries.

The Hanna Formation eventually buried the nose of Simpson Ridge anticline, and formed a continuous sheet of sandstone that joined the Hanna and Carbon basins. Calcite-cemented concretions grew in this sheet; many pipe-like calcite concretions grew parallel to the NW–SE direction of groundwater flow The sandstone sheet was gently folded before deformation ceased, and later erosion has divided it into western and eastern portions.

Early diagenetic concretions are commonly reworked in sedimentary systems, and, we argue here that, due to convergent groundwater flow, concretions—both *in situ* and as reworked clasts—may be especially likely to be found in syntectonic growth strata.

Siderite concretions in sandstone–siltstone outcrops are commonly completely altered to iron oxide, but siderite concretions in tight, carbon-rich claystones, even when uplifted and exposed to similar climatic conditions, are completely preserved. The oxidized remains of siderite concretions are distinctive, visually prominent, and highly informative. In meandering fluvial systems, early siderite concretions are commonly reworked by autocyclic processes (Loope et al. 2012; Burgess et al. 2016). This study demonstrates that reworked, iron-rich concretions can also reveal the interplay of deposition, early diagenesis, and erosion in tectonically active areas.

SUPPLEMENTAL MATERIAL

Paleocurrent diagrams are available from JSR's Data Archive: http://sepm.org/pages.aspx?pageid=229.

ACKNOWLEDGMENTS

Jay Lillegraven's (2015) meticulously detailed, two-decades-in-the-making grand opus greatly aided our short-term, specialized project; we believe good friends can come to different conclusions from the same outcrops. We thank Mike Leite, Jim Schmitt, and Paul McCarthy for their insightful reviews. We also thank Don Boyd for good advice, Anthony Kohtz and Cindy Loope for assistance in the field, and Anton Wroblewski, Peter Mozley, and Vitaly Zlotnik for helpful discussions.

REFERENCES

ALLEN, J.R.L., 1987, Reworking of muddy intertidal sediments in the Severn estuary, southwestern U.K.: preliminary survey: Sedimentary Geology, v. 50, p. 1–23.

AMBRAYSEYS, N., AND SARMA, S., 1969, Liquefaction in soils induced by earthquakes: International Association of Engineering Geology, Bulletin, v. 44, p. 5–16.

ARCHIBALD, J.D., GINGERICH, P.D., LINDSAY, E.H., CLEMENS, W.A., KRAUSE, D.W., AND ROSE, K.D., 1987, First North American land mammal ages of the Cenozoic Era, *in* Woodburne, M.O., ed., Cenozoic Mammals of North America, Geochronology and Biostratigraphy: Berkeley, University of California Press, p. 24–76.

ASCHOFF, J.L., AND SCHMITT, J.G., 2008, Distinguishing syntectonic unconformity types to enhance analysis of growth strata: an example from the Cretaceous, southeastern Nevada, U.S.A.: Journal of Sedimentary Research, v. 78, p. 608–623.

BERNER, R.A., 1971, Chemical Sedimentology: New York, McGraw-Hill, 240 p.

BERNER, R.A., 1981, A new geochemical classification of sedimentary environments: Journal of Sedimentary Petrology, v. 51, 359–365.

BLAIR, T.C., AND MCPHERSON, J.G., 1994, Alluvial fans and their natural distinction from rivers based on morphology, hydraulic processes, and facies assemblages: Journal of Sedimentary Research, v. 64, p. 450–489.

BLACKSTONE, D.L., JR., 1983, Laramide compressional tectonics, southeastern Wyoming: University of Wyoming, Contributions to Geology, v. 22, p. 1–38.

BLACKSTONE, D.L., JR., 1993, Overview of the Hanna, Carbon, and Cooper Lake Basins, Southeastern Wyoming: Geological Survey of Wyoming, Report of Investigations, No. 48, 20 p.

Blum, M., and Pecha, M., 2014, Mid-Cretaceous to Paleocene North American drainage reorganization from detrital zircons: Geology, v. 42, p. 607–610.

Boyd, D.W., and Lillegraven, J.A., 2011, Persistence of the Western Interior Seaway: historical background and significance of ichnogenus *Rhizocorallium* in Paleocene strata, south-central Wyoming: Rocky Mountain Geology, v. 46, p. 43–69.

Burbank, D.W., Meigs, A., and Brozovic, N., 1996, Interactions of growing folds and coeval depositional systems: Basin Research, v. 8, p. 199–223.

Burgess, D.T., Kettler, R.M., and Loope, D.B., 2016, The geologic context of wonderstone: a complex, outcrop-scaled pattern of iron-oxide cement: Journal of Sedimentary Research, v. 86, p. 498–511.

Cavazza, W., Braga, R., Reinhardt, E.G., and Zanotti, C., 2009, Influence of host-rock texture on the morphology of carbonate concretions in a meteoric diagenetic environment: Journal of Sedimentary Research, v. 79, p. 377–388.

Curtis, C.D., and Coleman, M.L., 1986, Controls on the precipitation of early diagenetic calcite, dolomite, and siderite concretions in complex depositional sequences, *in* Gautier, D.L., ed., Roles of Organic Matter in Sediment Diagenesis: SEPM, Special Publication 38, p. 23–33.

Davis, S.J., Dickinson, W.R., Gehrels, G.E, Spencer, J.E., Lawton, T.F., and Carroll, A.R., 2010, The Paleogene California River: evidence of Mojave–Uinta paleodrainage from U-Pb ages of detrital zircons: Geology, v. 38, p. 931–934.

Eberle, J.J., and Lillegraven, J.A., 1998a, A new important record of earliest Cenozoic mammalian history: geologic setting, Multituberculata, and Peradectia: Rocky Mountain Geology, v. 33, p. 3–47.

Eberle, J.J., and Lillegraven, J.A., 1998b, A new important record of earliest Cenozoic mammalian history: Eutheria and paleogeographic/biostratigraphic summaries: Rocky Mountain Geology, v. 33, p. 49–117.

Freeze, R.A., and Cherry, J.A., 1979, Groundwater: Englewood Cliffs, N.J., Prentice-Hall, 604 p.

Gautier, D.L., 1982, Siderite concretions: indicators of early diagenesis in the Gammon Shale (Cretaceous): Journal of Sedimentary Petrology, v. 52, p. 859–871.

Hall, J.S., Mozley, P.S., David, J.M., and Roy, N.D., 2004, Environments of formation and controls on spatial distribution of calcite cementation in Plio-Pleistocene fluvial deposits, New Mexico, USA: Journal of Sedimentary Research, v. 74, p. 643–653.

Hansen, D.E., 1986, Laramide tectonics and deposition of the Ferris and Hanna formations, south-central Wyoming, *in* Peterson, J.A., ed., Paleotectonics and Sedimentation in the Rocky Mountain Region, United States: American Association of Petroleum Geologists, Memoir 41, p. 481–495.

Hasiotis, S.T., and Honey, J.G., 2000, Paleohydrologic and stratigraphic significance of crayfish burrows in continental deposits: examples from several Paleocene Laramide basins in the Rocky Mountains: Journal of Sedimentary Research, v. 70, p. 127–139.

Keller, E.A., Zepeda, R.L., Rockwell, T.K., Ku, T.L., and Dinklage, W.S., 1998, Active tectonics at Wheeler Ridge, southern San Joaquin Valley, California: Geological Society of America, Bulletin, v. 110, p. 298–310.

Kettler, R.M., Loope, D.B., Weber, K.A., and Niles, P.B., 2015, Life and Liesegang: outcrop-scale microbially induced diagenetic structures and geochemical self-organization phenomena produced by oxidation of reduced iron: Astrobiology, v. 15, p. 616–636.

Lefebre, G.B., 1988, Tectonic evolution of the Hanna Basin, Wyoming: Laramide block rotation in the Rocky Mountain foreland [Ph.D. thesis]: Laramie, University of Wyoming, 240 p.

Lillegraven, J.A., 2015, Late Laramide tectonic fragmentation of the eastern greater Green River Basin, Wyoming: Rocky Mountain Geology, v. 50, p. 30–118.

Lillegraven, J.A., and Ostresh, L.M., 1988, Evolution of Wyoming's early Cenozoic topography and drainage: National Geographic Research, v. 4, p. 303–327.

Lillegraven, J.A., Snoke, A.W., and McKenna, M.C., 2004, Tectonic and paleogeographic implications of late Laramide geologic history in the northeastern corner of Wyoming's Hanna Basin: Rocky Mountain Geology, v. 39, p. 7–64.

Lofgren, D.L., Lillegraven, J.A., Clemens, W.A., Gingerich, P.D., and Williamson, T.E., 2004, Paleocene biochronology of North America: the Puercan through Clarkforkian land mammal ages, *in* Woodburne, M.O., ed., Late Cretaceous and Cenozoic Mammals of North America: Biostratigraphy and Geochronology: New York, Columbia University Press, p. 43–105.

Loope, D.B., and Kettler, R.M., 2015, The footprints of ancient CO_2-driven flow systems: ferrous carbonate concretions below bleached sandstone: Geosphere, v. 11, p. 943–957.

Loope, D.B., Kettler, R.M., and Weber, K.A., 2010, Follow the water: connecting a CO_2 reservoir and bleached sandstone to iron-rich concretions in the Navajo Sandstone of south-central Utah, USA: Geology, v. 38, p. 999–1002.

Loope, D.B., Kettler, R.M., and Weber, K.A., 2011, Morphologic clues to the origins of iron oxide-cemented spheroids, boxworks, and pipelike concretions, Navajo Sandstone of south-central Utah, U.S.A.: Journal of Geology, v. 119, p. 505–520.

Loope, D.B., Kettler, R.M., Weber, K.A., Hinrichs, N.L., and Burgess, D.T., 2012, Rinded iron-oxide concretions: hallmarks of altered siderite masses of both early and late diagenetic origin: Sedimentology, v. 59, p. 1769–1781.

Love, J.D., 1970, Cenozoic geology of the Granite Mountains area, central Wyoming: U.S. Geological Survey, Professional Paper 495C, 154 p.

Ludvigson, G.A., Gonzalez, L.A., Metzger, R.A., Witzke, B.J., Brenner, R.L., Murillo, A.P., and White, T.S., 1998, Meteoric spherosiderite lines and their use for paleohydrology and paleoclimatology: Geology, v. 26, p. 1039–1042.

Ludvigson, G.A., Witzke, B.J., Joeckel, R.M., Ravn, R.L., Phillips, P.L., Gonzalez, L.A., and Brenner, R.L., 2010, New insights on the sequence stratigraphic architecture of the Dakota Formation in Kansas–Nebraska–Iowa from a decade of sponsored research activity: Current Research in Earth Sciences, Bulletin 258, Part 2, 35 p.

Merewether, E.A., 1983, The Frontier Formation and mid-Cretaceous orogeny in the foreland of southwestern Wyoming: The Mountain Geologist, v. 20, p. 121–138.

Mozley, P.S., 1989, Relation between depositional environment and the elemental composition of early diagenetic siderite: Geology, v. 17, p. 704–706.

Mozley, P.S., and Davis, J.M., 1996, Relationship between oriented calcite concretions and permeability correlation structure in an alluvial aquifer, Sierra Ladrones Formation, New Mexico: Journal of Sedimentary Research, v. 66, p. 11–16.

Mozley, P.S., Beckner, J., and Whitworth, T.M., 1995, Spatial distribution of calcite cement in the Santa Fe Group, Albuquerque Basin, NM: implications for ground-water resources: New Mexico Geology, v. 17, p. 88–93.

Ogg, J.G., 2012, Geomagnetic Polarity Time Scale, *in* Gradstein, F.M., Ogg, J.G., Schmitz, M., and Ogg, G., eds., The Geologic Time Scale 2012: Boston, Elsevier, p. 85–113.

Pye, K., Dickson, J.A.D., Schiavon, N., Coleman, M.L., and Cox, M., 1990, Formation of siderite–Mg-calcite–iron sulfide concretions in intertidal marsh and sandflat sediments, north Norfolk, England: Sedimentology, v. 37, p. 325–343.

Ryan, J.D., 1977, Late Cretaceous and early Tertiary provenance and sediment dispersal, Hanna and Carbon basins, Carbon County, Wyoming: The Geological Survey of Wyoming, Preliminary Report, no. 16, 17 p.

Secord, R., 1996, Paleocene mammalian biostratigraphy of the Carbon Basin, southeastern Wyoming, with age constraints on local tectonism [Unpublished M.S. thesis]: Laramie, University of Wyoming, 184 p.

Secord, R., 1998, Paleocene mammalian biostratigraphy of the Carbon Basin, southeastern Wyoming, and age constraints on local phases of tectonism: Rocky Mountain Geology, v. 33, p. 119–154.

Secord, R., 2008, The Tiffanian land-mammal age (middle and late Paleocene) in the northern Bighorn Basin, Wyoming: The University of Michigan, Papers on Paleontology, v. 35, p. 1–192.

Secord, R., Gingerich, P.D., Smith, M.E., Clyde, W.C., Wilf, P., and Singer, B.S., 2006, Geochronology and mammalian biostratigraphy of middle and upper Paleocene continental strata, Bighorn Basin, Wyoming: American Journal of Science, v. 306, p. 211–245.

Schultz, C.B., 1941, The pipy concretions of the Arikaree: University of Nebraska State Museum, Bulletin, v. 2, p. 69–82.

Sharman, G.R., Covault, J.A., Stockli, D.F., Wroblewski, A.F.J., and Bush, MA., 2017, Early Cenozoic drainage reorganization of the United States Western Interior: Gulf of Mexico sediment routing system: Geology, v. 45, p. 187–190.

Suppe, J., Chou, G.T., and Hook, S.C., 1992, Rates of folding and faulting determined from growth strata, *in* McClay, K.R., ed., Thrust Tectonics: London, Chapman and Hall, p. 105–122.

Talling, P.J., and Sowter, M.J., 1999, Drainage density on progressively tilted surfaces with different gradients, Wheeler Ridge, California: Earth Surface Processes and Landforms, v. 24, p. 809–824.

Taylor, J.H., 1949, Petrology of the Northampton sand ironstone formation: Geological Survey of Great Britain, Memoir, 111 p.

van der Burg, W.J., 1969, The formation of rattle stones and the climatological factors which limited their distribution in the Dutch Pleistocene. 1. The formation of rattle stones: Palaeogeography, Palaeoclimatology, Palaeoecology, v. 6, p. 105–124.

Weber, K.A., Spanbauer, T.L., Wacey, D., Kilburn, M.R., Loope, D.B., and Kettler, R.M., 2012, Biosignatures link microorganisms to iron mineralization in a paleoaquifer: Geology, v. 40, p. 747–750.

Wroblewski, A.F.-J., 2003, Tectonic redirection of Paleocene fluvial drainage systems and lacustrine flooding in the Hanna Basin area, south-central Wyoming, *in* Raynolds, R.G., and Flores, R.M., eds., Cenozoic Systems of the Rocky Mountain Region: SEPM, Rocky Mountain Section, p. 227–252.

Wroblewski, A.F.-J., 2006, Relative influences of tectonism, climate, and sea level on valley incision and sedimentary fill: new insights from Upper Cretaceous and Paleocene examples, *in* Dalrymple, R.W., Leckie, D.A., and Tillman, R.W., eds., Incised Valleys in Time and Space: SEPM, Special Publication 85, p. 309–326.

Received 18 October 2016; accepted 27 June 2017.